

# Planar Glide-Symmetric Dielectric Half-Luneburg Lens at $K/K_a$ -Band

Oskar Zetterstrom\*, Pilar Castillo-Tapia\*, Jose-Manuel Poyanco†, Nelson J. G. Fonseca‡, Francisco Pizarro§ Oscar Quevedo-Teruel\*

\*Division of Electromagnetic Engineering, KTH Royal Institute of Technology, Stockholm, Sweden

†Department of Signal Theory and Communications, University Carlos III of Madrid, Leganés, Spain

‡Antenna and Sub-Millimetre Waves Section, European Space Agency, Noordwijk, The Netherlands

§Escuela de Ingeniería Eléctrica, Pontificia Universidad Católica de Valparaíso, Valparaíso, Chile

Email: oskarz@kth.se

**Abstract**—In this work, we design a planar half-Luneburg lens antenna. The gradient of refractive index is realized using a dielectric slab periodically loaded with air-cavities of varying size. The cavities are glide-symmetrically arranged. It is demonstrated that by introducing glide symmetry, the bandwidth and range of realizable refractive indices are increased compared to a non-glide-symmetric structure. The lens antenna operates from 22 to 32 GHz and can scan its directive beam over a 50 degree range in the H-plane. The side lobe level in this scan range is lower than -10 dB throughout the band.

**Index Terms**—Dielectric lens, glide symmetry, planar Luneburg lens

## I. INTRODUCTION

Antennas operating at high frequencies, typically  $K_u$ -band and above, are often required to provide a steerable and directive beam [1]. These properties can be obtained with conventional phased array antennas. However, at mm-wave frequencies, the feeding network for phased arrays can introduce prohibitive losses and be expensive. Quasi-optical systems are considered a promising alternative [2]. In particular, rotationally symmetric lenses can be used to design antennas with steerable directive beams.

One rotationally symmetric lens with attractive properties is the Luneburg lens [3]. A Luneburg lens is defined by the refractive index distribution

$$n(\rho) = n_0 \sqrt{2 - \frac{\rho^2}{R^2}}, \quad (1)$$

where  $n_0$ ,  $\rho$  and  $R$  are the refractive index of the surrounding medium, the radial position inside the lens, and the radius of the lens. The Luneburg lens transforms a cylindrical or spherical wave at its periphery into a quasi-planar wave at the opposite side of the lens. The refractive index varies smoothly in the lens and is matched to the surrounding medium (typically air) at the periphery of the lens. As a result, the Luneburg lens does not introduce reflections that deteriorate the performance of the antenna. On the other hand, the smoothly varying refractive index of the Luneburg lens can be difficult to realize.

The refractive index of the Luneburg lens can be realized using geodesic shapes or metasurfaces. In a geodesic Luneburg

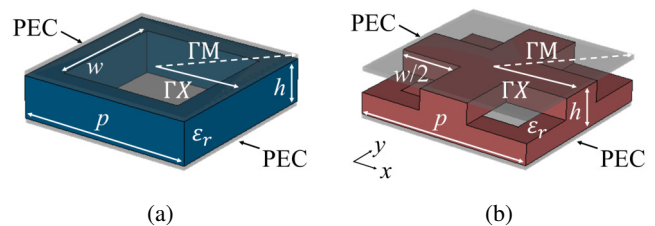


Fig. 1: Illustrations of the unit cells of the (a) conventional and (b) glide-symmetric periodic structures.

lens, the gradient of refractive index is mimicked by a deformed parallel plate waveguide (PPW) with a homogeneous medium inside [4], [5]. Typically, the lens is implemented in an empty ( $\epsilon_r = 1$ ) deformed PPW. It is noteworthy that the deformation of the waveguide increases the height of the antenna, and some recent works have investigated techniques to reduce this height [6]–[8]. In a metasurface Luneburg lens, the gradient of refractive index is mimicked with a quasi-periodic structure [9]–[11], and is typically implemented in a standard PPW. As a result, the lens can be planar. However, the manufacturing can be expensive [9], [10], and the bandwidth of the metasurface is often limited [9], [11].

Due to the rotational symmetry, a Luneburg lens antenna can steer its directive beam without scan losses. However, also due to the rotational symmetry, the aperture size scales with the focal length of the lens, which makes the device bulky. To reduce the size of the conventional Luneburg lens, the half-Luneburg lens was proposed [12], where a reflecting plane is used to reduce the size of the lens by a factor of 2. Note that the introduction of the reflecting surface brakes the rotational symmetry of the Luneburg lens. As a result, scan losses are expected. In [13], a geodesic half-Luneburg lens antenna is designed. It is demonstrated that a half-Luneburg lens antenna produces a maximum gain that is comparable to a conventional Luneburg lens antenna of the same size. The reported scan losses are roughly 3 dB when scanning  $\pm 30^\circ$  with respect to the centre beam.

In this work, we propose a metasurface half-Luneburg lens antenna that can be cost-effectively produced using additive

manufacturing. Furthermore, the proposed antenna can be planar and has a wide bandwidth. The design proposed shares some key parameters with that described in [14], thus facilitating the comparison between the standard Luneburg lens and the half-Luneburg lens solutions.

## II. GLIDE-SYMMETRIC DIELECTRIC HALF-LUNEBUG LENS ANTENNA

The lens is implemented in a PPW and the graded refractive index of the half-Luneburg lens is realized using a metasurface. In the following, we compare the response of a conventional

and glide-symmetric metasurface. We then use the glide-symmetric metasurface to design a half-Luneburg lens antenna.

### A. Glide-symmetric dielectric slab

A structure is glide-symmetric if it is invariant under a translation and a mirroring [15]–[19]. It has been demonstrated that glide-symmetric periodic structures can provide reduced frequency dispersion [9], and increased control of the anisotropy [9], [20] and effective refractive index [21], compared to conventional periodic structures. Fig. 1 illustrates the unit cells of the studied periodic structures. The dielectric slabs are illustrated in blue and red and are periodically loaded with air-cavities of widths  $w$  distributed in a square lattice with period  $p$  in the  $xy$ -plane. The dielectric slabs are placed between two metallic plates. The unit cell in Fig. 1b is a glide-symmetric counterpart to the unit cell in Fig. 1a. A similar unit cell is studied in [14], with the difference that the permittivity of the dielectric used in this work is  $\epsilon_r = 3$  as compared to  $\epsilon_r = 2.25$  in [14]. The use of a higher permittivity allows for a wider range of effective refractive indices, and thus enables a wider range of devices to be realized.

The effective refractive index of the two structures are presented in Fig. 2a for two widths of the air-cavities,  $w$ . The remaining parameters are  $p = 4.2$  mm and  $h = 2$  mm to ensure that the lens operates using the fundamental PPW mode up to 32 GHz. The effective refractive index is studied in two directions that are defined in Fig. 1. It is observed that for the same dimensions, the glide-symmetric structure provides a wider bandwidth and a lower effective refractive index. These properties are attractive for the design of a Luneburg lens since they alleviate the manufacturing. In other words, larger dimensions can be used to produce a lens using the glide-symmetric structure. Fig. 2b presents the effective refractive index at 20 GHz in the conventional and glide-symmetric structures as a function of the width of the air-cavity,  $w$ . The refractive index calculated as the volume ratio between the dielectric and air is included as reference. The effective refractive index in the glide-symmetric structure closely follows the calculation based on the volume ratio. In the design of the lens, we assume that the minimum wall width that can be manufactured is 0.4 mm. With this manufacturing constraint and using the glide-symmetric structure, a half-Luneburg lens can be realized by varying the widths of the cavities from 3.8 mm to 2.8 mm.

### B. Half-Luneburg lens antenna

The glide-symmetric structure is used to design a half-Luneburg lens antenna operating from 22 to 32 GHz. The radius of the lens is  $R = 50$  mm and it is fed with rectangular waveguides of size  $8.1 \times 2$  mm<sup>2</sup> placed at the contour of the lens. Seven waveguide feeds with an angular separation of  $10^\circ$  are used. It is noted that the bandwidth of the antenna is mainly limited by the feeding waveguides (not the lens). An exponential flare is used to match the impedance of the PPW to the free-space impedance. The height of the flare at

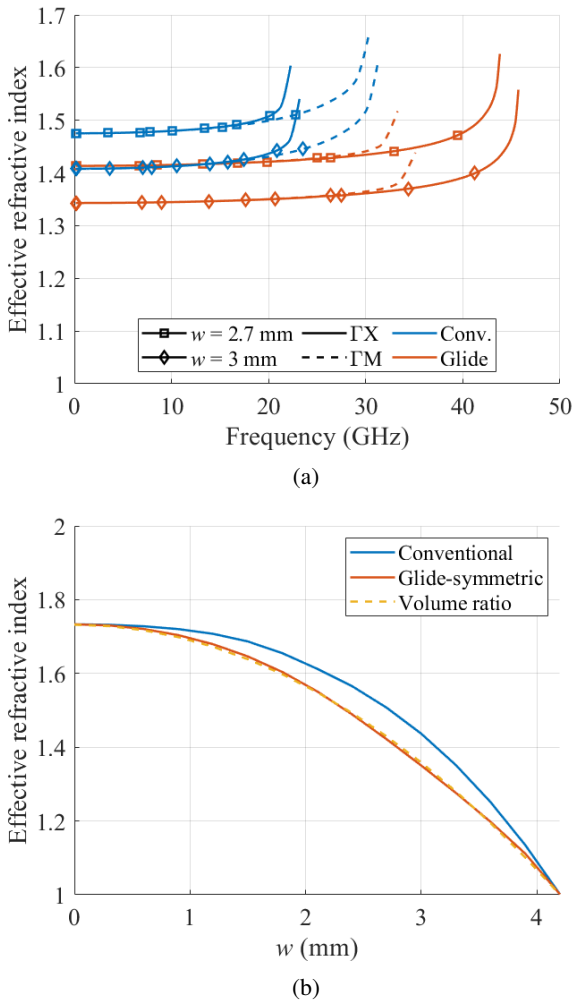


Fig. 2: (a) Comparison of the effective refractive index in the conventional and glide-symmetric structures for two sizes of cavities and propagation directions. The propagation directions are defined in Fig. 1. The dimensions are:  $p = 4.2$  mm,  $h = 2$  mm and  $\epsilon_r = 3$ . (b) Effective refractive index in the conventional and glide-symmetric structures at 20 GHz as a function of the cavity size. The refractive index calculated as the volume ratio between the dielectric and air is included as reference.

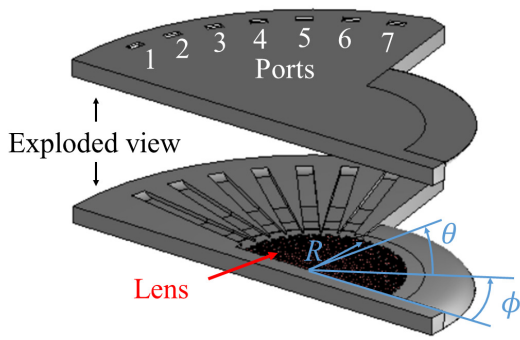


Fig. 3: Illustration of the designed lens antenna with the port numbers indicated.

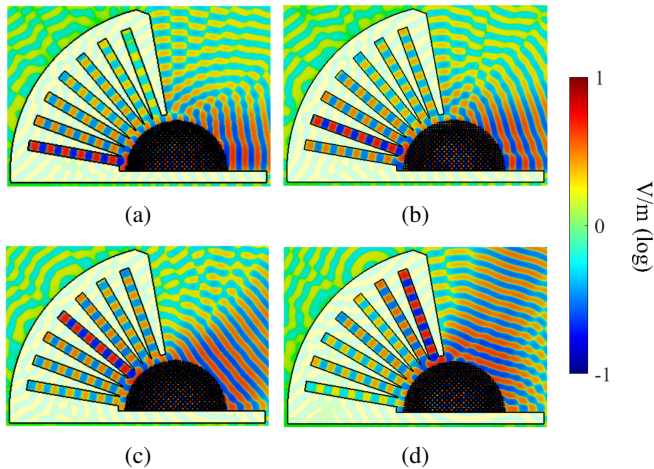
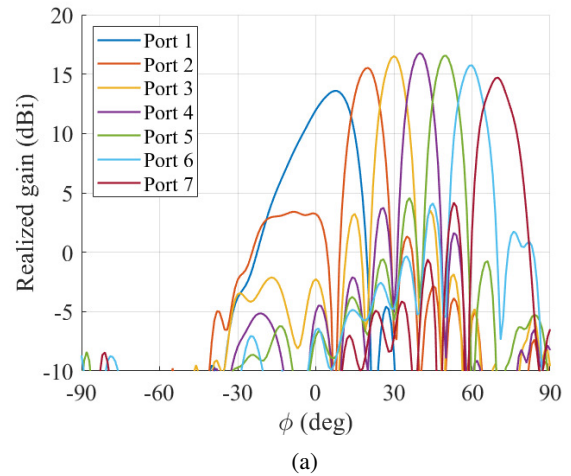


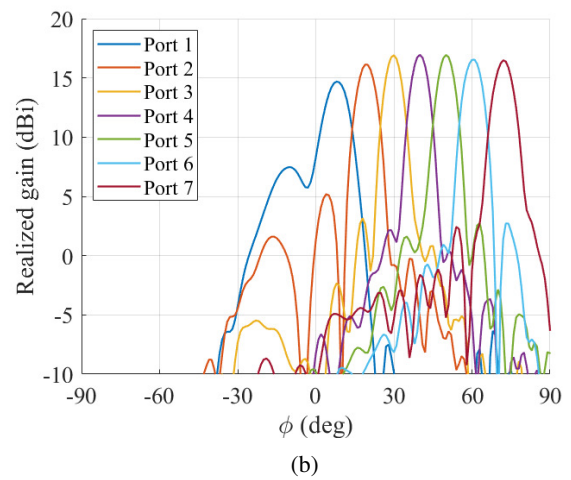
Fig. 4: Normalized electric field distribution in the lens antenna at 28 GHz when exciting waveguides: (a) 1, (b) 2, (c) 4, and (d) 7.

the output of the antenna is 17.5 mm. The lens antenna is illustrated in Fig. 3.

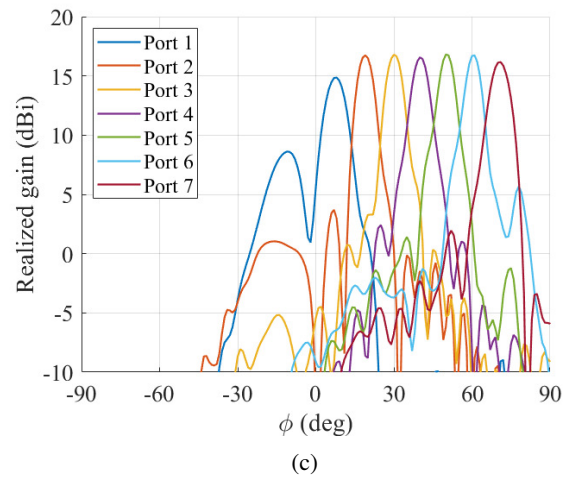
Fig. 4 presents the electric field distributions in the lens antenna when waveguides 1, 2, 4, and 7 are excited. The lens transforms the radiation from the feed waveguides to quasi-planar waves, except for port 1 where aberrations are observed at the output of the antenna. These aberrations are caused by the finite size of the reflecting wall in the antenna [13]. The radiation patterns at 22, 28, and 32 GHz of the lens antenna are presented in Fig. 5. The E-plane radiation pattern for port 4 is presented in Fig. 6. It is demonstrated that the lens produces a steerable directive fan-shaped beam across a wide bandwidth. In [14], a conventional Luneburg lens antenna is designed using the same flare and a similar metasurface with the same radius as the half-Luneburg lens designed in this work. The achieved peak gain in the half-Luneburg lens antenna is roughly 1.5 dB smaller than the gain in the conventional Luneburg lens, although the half-Luneburg lens occupies only half the volume of the conventional Luneburg



(a)



(b)



(c)

Fig. 5: Simulated H-plane radiation pattern at (a) 22 GHz, (b) 28 GHz, and (c) 32 GHz.

lens. It is noted that, for the center beam half-Luneburg lens antenna, the aperture is only slightly smaller than the one in the conventional Luneburg lens antenna. For the scanned beams in the half-Luneburg lens antenna, the gain is reduced due to the

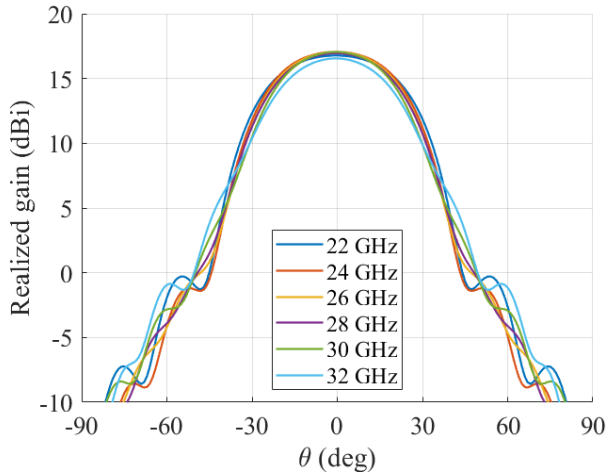


Fig. 6: E-plane radiation pattern for port 4.

smaller aperture size, compared to the conventional Luneburg lens antenna. Furthermore, significant side lobes appear in the radiation pattern for port 1. These side lobes are a result of the aforementioned aberrations. This effect can be reduced by extending the reflecting wall, which comes at the cost of size of the antenna. The scan losses in the half-Luneburg lens are less than 1.5 dB when scanning from  $\phi = 20^\circ$  to  $\phi = 70^\circ$ .

### III. CONCLUSIONS

In this work, we presented a half-Luneburg lens antenna operating from 22 to 32 GHz. The refractive index distribution of the lens is realized using a dielectric slab that is periodically loaded with glide-symmetric air-cavities. Importantly, we compared the effective refractive indices produced by a glide-symmetric and conventional structure. From this comparison, we observed that glide symmetry can be used to increase the bandwidth and alleviate the manufacturing of the lens. This allowed for the realization of a larger range of refractive indices at a lower cost. The lens was fed with seven rectangular waveguides placed at the periphery of the lens. The resulting antenna can steer its directive radiation in one plane in a  $50^\circ$  range. The antenna has at most 1.5 dB scan losses in this range throughout the band. These are encouraging results considering the significant size reduction. The lens can be manufactured using additive manufacturing.

### ACKNOWLEDGEMENT

This work has been partly funded by the strategic innovation program Smarter Electronics System under project High-Int (2019-02103). The work of O. Quevedo-Teruel and P. Castillo-Tapia was also funded by the VR Project 2019-03933. The work of O. Zetterstrom was funded by the ESA ARTES contract 4000125905/18/NL. The work of J.M. Poyanco and F. Pizarro was funded by the Chilean project ANID PCI-MEC 8019007.

### REFERENCES

- [1] Y. Wang, J. Li, L. Huang, Y. Jing, A. Georgakopoulos, and P. Demestichas, "5G mobile: Spectrum broadening to higher-frequency bands to support high data rates," *IEEE Veh. Technol. Mag.*, vol. 9, no. 3, pp. 39–46, Sep. 2014.
- [2] Y. J. Guo, M. Ansari, R. W. Ziolkowski, and N. J. G. Fonseca, "Quasi-optical multi-beam antenna technologies for 5G and 6G mmWave and THz networks: A review," *IEEE Open J. Antennas Propag.*, vol. 2, pp. 807–830, June 2021.
- [3] R. Luneburg, "Mathematical theory of optics," *Brown University Press, Providence, RI*, pp. 208–213, 1944.
- [4] R. F. Rinehart, "A solution of the problem of rapid scanning for radar antennae," *J. Appl. Phys.*, vol. 19, p. 860–862, Sept. 1948.
- [5] —, "A family of designs for rapid scanning radar antennas," *Proc. IRE*, vol. 40, p. 686–688, June 1952.
- [6] Q. Liao, N. Fonseca, and O. Quevedo-Teruel, "Compact multibeam fully metallic geodesic Luneburg lens antenna based on non-Euclidean transformation optics," *IEEE Trans. Antennas Propag.*, vol. 66, no. 12, pp. 7383–7388, Dec. 2018.
- [7] N. J. G. Fonseca, Q. Liao, and O. Quevedo-Teruel, "Equivalent planar lens ray-tracing model to design modulated geodesic lenses using non-Euclidean transformation optics," *IEEE Trans. Antennas Propag.*, vol. 68, no. 5, pp. 3410–3422, May 2020.
- [8] N. J. G. Fonseca, "The water drop lens: revisiting the past to shape the future," *EurAAP Reviews Electromag.*, vol. 1, no. 1, pp. 1–4, Sept. 2021.
- [9] O. Quevedo-Teruel, J. Miao, M. Mattsson, A. Algaba-Brazalez, M. Johansson, and L. Manholm, "Glide-symmetric fully metallic Luneburg lens for 5G communications at Ka-band," *IEEE Antennas Wireless Propag. Lett.*, vol. 17, no. 9, pp. 1588–1592, Sept. 2018.
- [10] H. Lu, Z. Liu, Y. Liu, H. Ni, and X. Lv, "Compact air-filled Luneburg lens antennas based on almost-parallel plate waveguide loaded with equal-sized metallic posts," *IEEE Trans. Antennas Propag.*, vol. 67, no. 11, pp. 6829–6838, Nov. 2019.
- [11] O. Zetterstrom, R. Hamarneh, and O. Quevedo-Teruel, "Experimental validation of a metasurface Luneburg lens antenna implemented with glide-symmetric substrate-integrated-holes," *IEEE Antennas Wireless Propag. Lett.*, vol. 20, no. 5, pp. 698–702, May. 2021.
- [12] J. Sanford, "A Luneburg-lens update," *IEEE Antennas Propag. Mag.*, vol. 37, no. 1, pp. 76–79, 1995.
- [13] N. J. G. Fonseca, Q. Liao, and O. Quevedo-Teruel, "Compact parallel-plate waveguide half-Luneburg geodesic lens in the Ka-band," *IET Microw. Antennas Propag.*, vol. 15, no. 2, pp. 123–130, Feb. 2021.
- [14] J.-M. Poyanco, O. Zetterstrom, P. Castillo-Tapia, N. J. G. Fonseca, F. Pizarro, and O. Quevedo-Teruel, "Two-dimensional glide-symmetric dielectric structures for planar graded-index lens antennas," (*early access*) *IEEE Antennas Wirel. Propag. Lett.*, 2021.
- [15] P. J. Crepeau and P. R. McIsaac, "Consequences of symmetry in periodic structures," *Proc. IEEE*, vol. 52, no. 1, pp. 33–43, Jan 1964.
- [16] R. Mittra and S. Laxpati, "Propagation in a wave guide with glide reflection symmetry," *Can. J. Phys.*, vol. 43, no. 2, pp. 353–372, 1965.
- [17] R. Kiebertz and J. Impagliazzo, "Multimode propagation on radiating traveling-wave structures with glide-symmetric excitation," *IEEE Trans. Antennas Propag.*, vol. 18, no. 1, pp. 3–7, Jan 1970.
- [18] A. Hessel, M. H. Chen, R. C. M. Li, and A. A. Oliner, "Propagation in periodically loaded waveguides with higher symmetries," *Proc. IEEE*, vol. 61, no. 2, pp. 183–195, Feb 1973.
- [19] O. Quevedo-Teruel, Q. Chen, F. Mesa, N. J. G. Fonseca, and G. Valerio, "On the benefits of glide symmetries for microwave devices," *IEEE J. Microwaves*, vol. 1, no. 1, pp. 457–469, 2021.
- [20] M. Ebrahimpouri and O. Quevedo-Teruel, "Ultrawideband anisotropic glide-symmetric metasurfaces," *IEEE Antennas Wireless Propag. Lett.*, vol. 18, no. 8, pp. 1547–1551, Aug 2019.
- [21] P. Arnberg, O. Barreira Petersson, O. Zetterstrom, F. Ghasemifard, and O. Quevedo-Teruel, "High refractive index electromagnetic devices in printed technology based on glide-symmetric periodic structures," *Appl. Sci.*, vol. 10, no. 9, 2020.